# The Environmental Toxicant 2,3,7,8-Tetrachlorodibenzo-*p*-Dioxin Disturbs the Establishment and Maintenance of Cell Polarity in Preimplantation Rat Embryos[1]

**Karla J. Hutt,**[3,4] **Zhanquan Shi,**[3,5] **Brian K. Petroff,**[3,5] **and David F. Albertini**[2,3,4,6]

*The Center for Reproductive Sciences,*[3] *Department of Molecular and Integrative Physiology,*[4] *and Department of Internal Medicine,*[5] *University of Kansas Medical Center, Kansas City, Kansas*
*Marine Biological Laboratory,*[6] *Woods Hole, Massachusetts*

## ABSTRACT

Maternal exposure to the environmental toxicant 2,3,7,8-tetrachlorodibenzo-*p*-dioxin (TCDD) induces a variety of defects in compaction-stage embryos, including monopolar spindle formation, errors in chromosome segregation, and fragmentation resulting from aberrant cytokinesis. In this study, we investigated the possibility that a failure in centrosome duplication, separation, or positioning within blastomeres might underlie the observed effects of TCDD on early embryos. The subcellular localization of the centrosomal marker TUBG1 was analyzed in preimplantation embryos collected from female rats exposed to either chronic (50 ng kg$^{-1}$ wk$^{-1}$ for 3 wk) or acute (50 ng/kg or 1 μg/kg at proestrus) doses of TCDD. In treated embryos, interphase TUBG1 foci were more abundant and cortically displaced when compared to those in controls. At prophase, some blastomeres exhibited a single large perinuclear TUBG1 aggregate, suggesting a failure in centrosome duplication or separation. Furthermore, the presence of monopolar spindles at metaphase was confirmed by the localization of TUBG1 to the single spindle pole. Therefore, the misregulation of centrosome number and localization, as indicated by TUBG1 staining, may contribute to errors in chromosome segregation and cytokinesis in embryos following maternal TCDD exposure.

*cell cycle, centrosome, dioxin, early development, embryo, spindle, toxicology, tubulin*

## INTRODUCTION

Centrosomes are the organelles responsible for nucleating microtubules. In most cells, centrosomes are comprised of a pair of centrioles surrounded by pericentriolar material. However, the centrosomes of the oocyte and early embryo do not contain centrioles [1, 2]. In these cells, aggregates of pericentriolar material provide functional microtubule organizing centers capable of assembling interphase microtubule networks as well as bipolar spindles. A conserved member of the tubulin superfamily, TUBG1 (γ-tubulin) is a key component of the pericentriolar material. Most TUBG1 is found as the γ-tubulin ring complex, which nucleates microtubule assembly and acts as a minus end capping protein [3, 4]. Additionally, roles have been established for TUBG1 in the maintenance of interphase microtubule dynamics [5], spindle assembly and function [5, 6], cell-cycle checkpoint regulation [7], and chromosome-to-pole movement during anaphase [8–11]. Recent evidence also shows that centrosomes provide a scaffold for accumulation of numerous regulatory proteins, especially those that are exchanged between the cytoplasm and nucleus [12].

Centrosome number, position, and function are cell-cycle dependent. Cells in the $G_1$ phase of the cell cycle have a single small centrosome [13]. At the $G_1$/S transition, Cdk2/cyclin E or cyclin A activity induces centrosomes duplication [14, 15]. By the M phase, each centrosome has acquired the maximal amount of pericentriolar material, and the two centrosomes separate in early mitosis to participate in spindle pole formation [16–18]. To ensure appropriate bipolar spindle assembly, cytokinesis, and chromosome segregation, it is essential that centrosomes duplicate only once during each cell cycle. Defects in centrosome duplication and function are associated with human diseases, including cancer.

The aryl hydrocarbon receptor (AHR) is a transcription factor that mediates the effects of environmental pollutants belonging to the halogenated aromatic hydrocarbon family, such as 2,3,7,8-tetrachlorodibenzo-*p*-dioxin (TCDD). TCDD is an extremely potent toxicant that contaminates the environment as a consequence of waste incineration, industrial processes, and past herbicide use. Numerous studies have shown that TCDD causes adverse effects on both animal and human health by disrupting endocrine homeostasis, cellular proliferation, and tissue differentiation and is associated with birth defects, infertility, and cancer [19–21]. Ligand-bound AHR translocates to the nucleus and binds with ARNT to form an active transcription complex that interacts with the dioxin-responsive element present in the promoter region of AHR-regulated genes to control their transcription [22]. In addition to its activity as a transcriptional regulator, AHR influences diverse cellular processes by modifying protein phosphorylation signaling events [23].

Recently, we showed in rats that maternal exposure to environmentally relevant doses of TCDD disrupts compaction-stage embryonic development but does not prevent survival to the blastocyst stage [24]. In particular, TCDD was found to induce the formation of monopolar spindles. In the present study, we aimed to further understand the mechanism by which TCDD disrupts mitotic spindle formation in cleavage-stage embryos. For this purpose, we used high-resolution confocal microscopy to characterize the effects of chronic and acute maternal TCDD exposure on the following: 1) subcellular TUBG1 foci number and position, 2) mitotic spindle integrity, 3) nuclear position, and 4) f-actin organization from the time of compaction through the early blastocyst stage.
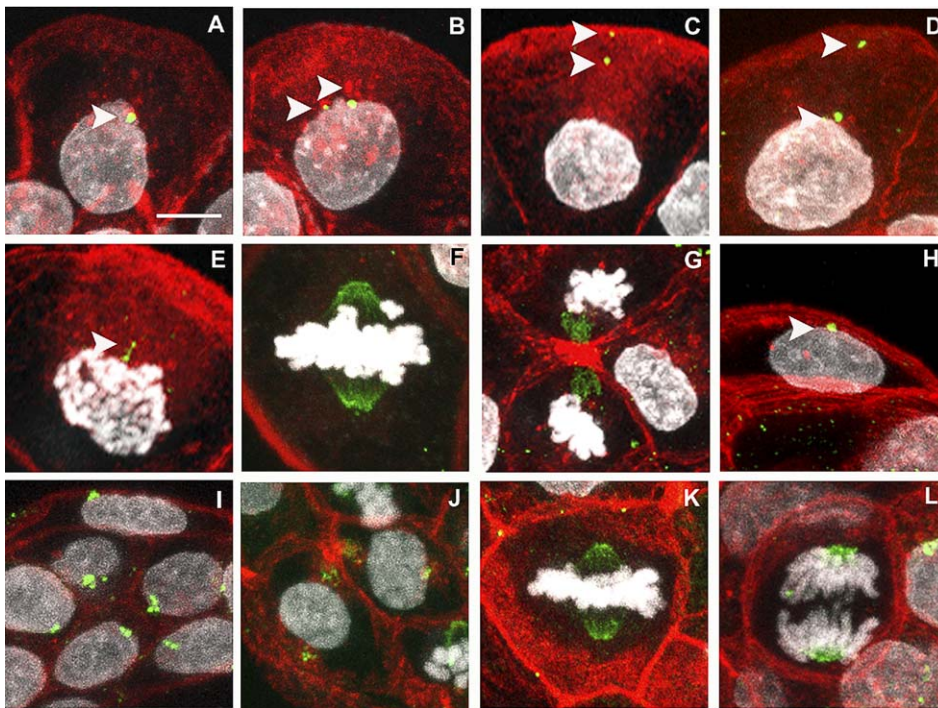
FIG. 1. Localization of TUBG1 in rat pre-implantation embryos. Eight- to 16-cell embryos (A–G) and blastocysts (H–J) were stained for visualization of TUBG1 (green), f-actin (red), and DNA (white). At the 8- to 16-cell stage, interphase blastomeres exhibited one or two TUBG1 foci with perinuclear or cortical positioning (A–D, arrows). TUBG1 was also localized to spindle poles and midbodies of mitotic blastomeres (E–G). In blastocysts, aggregates of TUBG1 were observed in TE (H) and ICM (J) cells and at the spindle at metaphase (K) and chromosomes at anaphase (L). Bar = 10 µm.

## MATERIALS AND METHODS

### Animals

Female Sprague-Dawley rats (Charles River Laboratories) were housed under a 12L:12D photoperiod at an ambient temperature of 23 ± 2°C with food and water ad libitum. All procedures were approved by the University of Kansas Medical Center Institutional Animal Care and Use Committee. The estrous cycle of rats was monitored by vaginal cytology. The normal estrous cycle of the rat has a duration of 4–5 days and exhibits a characteristic cyclic sequence of vaginal cytologic changes.

In experiment 1 (chronic exposure), female Sprague-Dawley rats were exposed chronically to TCDD beginning in utero. Given that TCDD has a long half-life in the rat (3 wk), a weekly dosing regime was employed. Initially, pregnant dams (n = 3 for each experimental group) received an oral dosing of TCDD (50 ng/kg) or corn oil vehicle (4 ml/kg) on Gestational Days 14 and 21 and then on Postpartum Days 7 and 14 to provide in utero and postnatal lactational exposure, respectively. On Postnatal Day 21, female offspring (n = 3 per experimental group) were weaned and orally dosed with TCDD (50 ng/kg) or corn oil vehicle (4 ml/kg), and dosing was continued at weekly intervals thereafter. This dose mimics the repeated exposures of people in high-risk occupations or contaminated environments. At 3 mo of age, proven males were introduced on the evening of proestrus, and breeding was confirmed by the presence of sperm on vaginal cytology the following morning. Embryos were collected in FHM medium (Chemicon) prewarmed to 37°C by flushing oviducts and uteri on Day 4.5 after coitus.

In experiment 2 (acute periconceptional exposure), female Sprague-Dawley rats (n = 3–6 for each experimental group) received a single oral dose (50 ng/kg or 1 µg/kg) of TCDD (Chemical Abstracts Service no. AS 1746-01-6; molecular weight, 321.9; purity, >99%) or corn oil vehicle (4 ml/kg) on the evening of proestrus and were housed with a male of proven fertility. At the time of dosing, rats were 50 days of age. The low dose mimics exposure of high-risk human populations, whereas the high dose is greater than the level in the majority of exposures. Breeding was confirmed by the presence of sperm on vaginal cytology the following morning. Embryos were collected in FHM medium prewarmed to 37°C by flushing oviducts and uteri on Day 4.5 or 5.5 after coitus.

### Immunofluorescence

Embryos were processed for TUBG1, DNA, and f-actin immunofluorescence as previously described [25]. Immediately following their collection, embryos were fixed for 30 min in 4% paraformaldehyde at 37°C and stored at 4°C in wash solution (PBS supplemented with 2% bovine serum albumin, 2% skim milk powder, 2% normal goat serum, 100 mM glycine, 0.01% Triton-X-

100, and 0.2% sodium azide) until processing for immunofluorescence. Embryos were extracted for 30 min at room temperature in 0.1% Triton-X-100 and incubated overnight at 4°C in wash solution. For immunostaining of microtubules, embryos were first incubated with mouse monoclonal anti-TUBG1 (Sigma) diluted 1:100 in wash solution for 1 h at 37°C, followed by Alexa 488-labeled goat anti-mouse IgG (Molecular Probes) diluted 1:1000 in wash solution for 1 h at 37°C. DNA was stained with Hoechst 33258 (1 µg/ml in wash solution) for 30 min, and cytoskeletal integrity was analyzed by staining f-actin with rhodamine-labeled phalloidin (1 µg/ml in wash solution; Molecular Probes) for 30 min. Embryos were mounted under cover slips without compression in medium containing 50% glycerol and 25 mg/ml of sodium azide.

Embryos were analyzed using a Zeiss LSM Pascal confocal imaging system mounted on a Zeiss Axioscope II with ultraviolet (405 nm), HeNe (543 nm), and argon (488 nm) laser excitation of probes. For every embryo, a complete z-axis data set was collected at 0.8-µm intervals (~50 sections/embryo) using a 63× oil objective (NA = 1.4). Laser power, gain, and offset settings were not changed between samples. All measurements, spatial restoration, and three-dimensional projections for each z-series data set were computed and analyzed using Zeiss LSM 5 Image Browser.

### Analysis of TUBG1 Foci Location

Eight- to 16-cell embryos were collected from control and exposed (50 ng kg$^{-1}$ wk$^{-1}$, 50 ng/kg, or 1 µg/kg of TCDD) female rats, and interphase blastomeres were assessed for the position of TUBG1 foci in relation to the nucleus. Blastomeres were classified as having foci at the nucleus only, at the cortex only, or at both the nucleus and cortex. Embryos were collected from at least three dams for each treatment group. The number of embryos in each treatment group was as follows: chronic control, n = 10; 50 ng kg$^{-1}$ wk$^{-1}$ of TCDD, n = 12; acute control, n = 12; 50 ng/kg of TCDD, n = 12; and 1 µg/kg of TCDD, n = 10. The number of blastomeres assessed was as follows: chronic control, n = 106; 50 ng kg$^{-1}$ wk$^{-1}$ of TCDD, n = 62; acute control, n = 128; 50 ng/kg of TCDD, n = 151; and 1 µg/kg of TCDD, n = 156. Fisher exact test was used to compare the number of blastomeres with TUBG1 foci at the nucleus or at the cortex between control and treated embryos. A value of $P < 0.05$ was considered to be a statistically significant difference.

### Analysis of Nuclear Location

Eight-cell embryos were collected from control and exposed (50 ng kg$^{-1}$ wk$^{-1}$, 50 ng/kg, or 1 µg/kg of TCDD) female rats and blastomeres (n = 48 blastomeres for each group, n = 6–8 blastomeres/embryo [only interphase blastomeres were assessed]; embryos were collected from at least three dams for each treatment group) were assessed for nuclear location. For this analysis,

TABLE 1. Location of TUBG1 foci in interphase blastomeres following chronic TCDD exposure.

| | Percentage of blastomeres (number) | | | |
|---|---|---|---|---|
| | Control (n = 106) | | 50 ng/kg/wk TCDD (n = 62) | |
| Location of γ-tubulin foci | | | | |
| Nucleus | 52 | (55) | 34 | (21)* |
| Cortex | 36 | (38) | 55 | (34)* |
| Nucleus and cortex | 12 | (13) | 11 | (7) |

* $P < 0.05$, Fisher exact test comparing the number of blastomeres in control and treated embryos with TUBG1 foci at the nucleus or at the cortex.

the shortest distance between the edge of the nucleus and the basal domain of the cell was measured using Zeiss Pascal software. Data were subjected to *t*-tests or one-way ANOVA by Tukey post hoc test. Mean, SEM, and minimum and maximum values are presented as box-and-whisker plots. A value of $P < 0.05$ was considered to be a statistically significant difference.

### Statistical Analysis

All statistical analysis was performed as described using Prism 4.08 (GraphPad Software, Inc.). For details of statistics, see the relevant section above.

## RESULTS

### Subcellular Localization of TUBG1 in 8- to 16-Cell Rat Pre-Embryos

Much of what is known about TUBG1 localization during early embryogenesis has come from studies of embryos derived from hormonally stimulated animals and/or in vitro embryo culture, which may not be representative of the true in vivo state. Therefore, we first examined TUBG1 localization within polarized blastomeres of compacted 8- to 16-cell embryos collected from naturally cycling and mated rats (Fig. 1, A–G). During interphase, TUBG1 was present as one or more discrete foci of varying sizes located immediately adjacent to the nucleus, at the cortex, or at both subcellular locations (Fig. 1, A–D). Foci were always oriented toward the apical free domain of each blastomere and were usually embedded within the polarized cytoplasmic f-actin-rich domain that extended from the nucleus to the apical surface. At prophase, two enlarged TUBG1 foci were detected in close proximity to the condensing chromosomes (Fig. 1E). When the chromosomes became aligned on a metaphase plate, TUBG1 was detected as intense staining at both poles of the pointed spindle and also on

the spindle microtubules (Fig. 1F). At early anaphase, TUBG1 was localized to the spindle adjacent to the chromosomes. However, during late anaphase/telophase, TUBG1 appeared within the interzone of the elongating spindle and was prominently localized to the midbody following cytokinesis (Fig. 1G). TUBG1 staining was not detected in approximately 20% of the interphase blastomeres analyzed.

### Subcellular Localization of TUBG1 in Rat Early Blastocysts

In trophectoderm (TE) cells of the rat early blastocyst (32 cells), one or two discrete TUBG1 foci were typically located adjacent to interphase nuclei (Fig. 1H). The foci were frequently located within an invagination of the nuclear envelope and were oriented toward the outer surface of the blastocyst. TUBG1 foci were not detected in approximately 20% of the TE cells analyzed. One or two large and slightly diffuse TUBG1 aggregates were detected within all cells of the inner cell mass (ICM) (Fig. 1, I and J). In these cells with little cytoplasm, the TUBG1 aggregates tended to be attached to the nucleus and also tethered to the membrane on either side of the nucleus, embedded within f-actin meshworks (Fig. 1J). As described above for the earlier-stage embryos, mitotic spindles at metaphase and anaphase, as well as midbodies of both TE and ICM, routinely stained for TUBG1 (Fig. 1, K and L).

### Chronic TCDD Exposure Modifies the Subcellular Localization of TUBG1 in 8- to 16-Cell Rat Pre-Embryos

We analyzed the subcellular location of TUBG1 in 8- to 16-cell rat pre-embryos following chronic maternal exposure to environmentally relevant doses of TCDD (50 ng $kg^{-1}$ $wk^{-1}$). Similar to controls, TUBG1 foci were detected at the nucleus, at the cortex, or at a combination of both positions in interphase blastomeres from TCDD-treated, 8- to 16-cell pre-embryos (Table 1). However, TUBG1 foci were more frequently detached from the nucleus and displaced toward the apical and/or outer regions of the blastomere cortex in treated pre-embryos when compared to controls ($P < 0.05$) (Table 1 and Fig. 2A, which shows one foci detached from the nucleus).

Whereas control blastomeres usually had one or two discrete foci, treated blastomeres often exhibited multiple foci distributed throughout the cytoplasm, indicative of fragmentation or deregulated replication (Fig. 2, A–D). Moreover, some prophase blastomeres exhibited a solitary large perinuclear TUBG1 aggregate (Fig. 2E), suggesting a possible failure in centrosome duplication or separation. In a number of metaphase-stage blastomeres, TUBG1 was only localized to a



FIG. 2. Localization of TUBG1 in rat preimplantation embryos following chronic maternal TCDD exposure. Eight- to 16-cell embryos (**A–H**) were collected from female rats chronically exposed to TCDD and stained for visualization of TUBG1 (green), f-actin (red), and DNA (white). Interphase blastomeres exhibited multiple TUBG1 foci (**A–D**, arrows). Some prophase blastomeres only had one foci (**E**). TUBG1 was also localized to a single spindle pole at metaphase, with foci detected in the cytoplasm but not contributing to the spindle (**F**, arrow). In some mitotic blastomeres, appropriate chromosome alignment (**G**) and segregation failed (**H**). Bar = 10 μm.
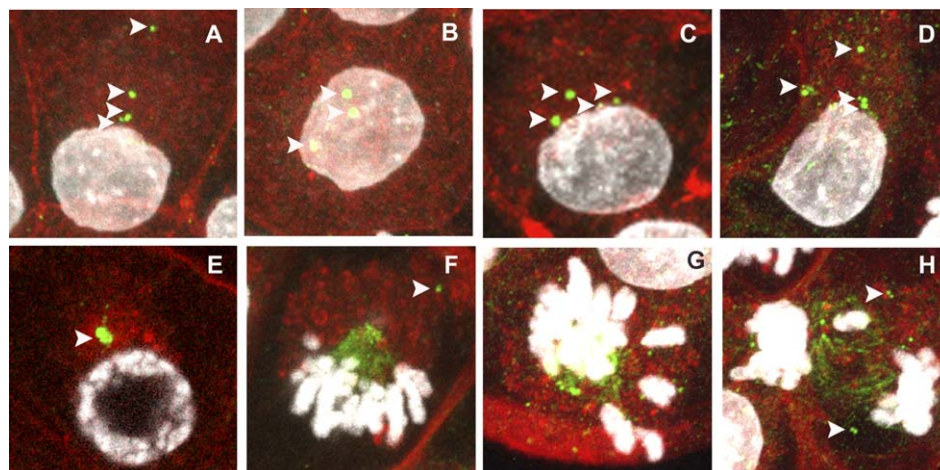
TABLE 2. Location of TUBG1 foci in interphase blastomeres following acute TCDD exposure.

| Location of TUBG1 foci | Percentage of blastomeres (number) | | | | | |
|---|---|---|---|---|---|---|
| | Control (n = 83) | | 50 ng/kg TCDD (n = 127) | | 1 μg/kg TCDD (n = 114) | |
| Nucleus | 78 | (65) | 48 | (61)* | 54 | (61)* |
| Cortex | 13 | (11) | 33 | (42)* | 31 | (36)* |
| Nucleus and cortex | 19 | (7) | 19 | (24) | 15 | (17) |

* $P < 0.05$; Fisher exact test comparing the number of blastomeres in control and treated (50 ng/kg or 1μg/kg TCDD) embryos with TUBG1 foci at the nucleus or at the cortex.

single spindle pole, which was oriented toward the apical domain of the cell cortex (Fig. 2, F and G). In dividing blastomeres, multiple TUBG1 foci were detected at the cortex spatially distinct from the mitotic spindle (Fig. 2F, arrow). In affected blastomeres, chromosomes were misaligned at the presumptive spindle equator, and monopolar spindles were basally displaced (Fig. 2G). This metaphase configuration was consistent with our previous result of monopolar spindle formation following TCDD exposure. Monopolar spindles were never observed in control embryos and were strictly a feature of the treated embryos in these experiments. Finally, chromosomes were detected within strands of TUBG1 between separating chromosomes at telophase (Fig. 2H). It was also noted that chromatin within telophase blastomeres frequently appeared to resemble a decondensation state typically found only following cytokinesis (9/10 treated telophase blastomeres vs. 0/7 control telophase blastomeres exhibited this phenomenon), suggesting that TCDD induced premature chromatin decondensation and cell-cycle asynchrony (Fig. 2H).

*Acute Periconceptional TCDD Exposure Modifies the Subcellular Localization of TUBG1 in 8- to 16-Cell Rat Pre-Embryos*

We next analyzed the subcellular localization of TUBG1 in 8- to 16-cell and blastocyst-stage rat pre-embryos following a single periconceptional dose (50 ng/kg and 1 μg/kg) of TCDD. Similar to the results obtained following chronic TCDD exposure, acute TCDD administration caused a displacement of TUBG1 foci from the nucleus to the blastomere cortex

(Table 2). In controls, approximately 80% of blastomeres demonstrated perinuclear TUBG1 foci, whereas only 50% of blastomeres from treated animals (50 ng/kg and 1 μg/kg) exhibited foci that approximated the nucleus. These displaced TUBG1 foci were sometimes detected outside of the f-actin-rich domain in which they typically reside within control embryos (not shown). Additionally, mitotic spindles from pre-embryos at both TCDD doses frequently exhibited TUBG1 staining at only one pole (for an example of a monopolar spindle, see Fig. 2F).

Interestingly, acute periconceptional TCDD exposure did not affect the subcellular localization of TUBG1 within TE or ICM from rat early blastocysts (not shown). However, TE of treated blastocysts frequently exhibited more than two TUBG1 foci (not shown).

*Chronic and Acute TCDD Exposure Modifies Nuclear Position in 8- to 16-Cell Rat Pre-Embryos*

During the present study, it became apparent that TCDD exposure not only modified the position of TUBG1 foci within blastomeres but also affected nuclear position. In control pre-embryos, nuclei were basally positioned and, on average, were located approximately 1.7 μm from the basal domain of the cell (Fig. 3). However, chronic exposure to TCDD caused nuclei to assume a more central location within blastomeres. In treated pre-embryos, nuclei were positioned an average of 3.5 μm from the basal domain of the cell (Fig. 3). The effect on nuclear displacement was recapitulated upon acute periconceptional exposure to TCDD, with nuclei located an average of 2.5, 4,
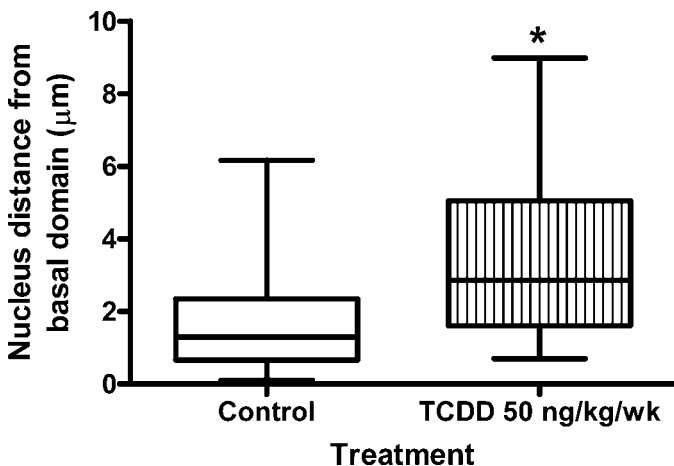
FIG. 3. Chronic maternal TCDD exposure modifies nuclear position in interphase blastomeres. Eight-cell embryos were collected from control and exposed (50 ng kg$^{-1}$ wk$^{-1}$ of TCDD) female rats, and interphase blastomeres (n = 48 blastomeres for each group) were assessed for the position of nuclei in relation to the basal domain of the cell. Asterisk (*) indicates a significant difference compared to controls ($P < 0.05$).

FIG. 4. Acute maternal TCDD exposure modifies nuclear position in interphase blastomeres. Eight-cell embryos were collected from control and exposed (50 ng/kg of 1 μg/kg of TCDD) female rats, and interphase blastomeres (n = 48 blastomeres for each group) were assessed for the position of nuclei in relation to the basal domain of the cell. Asterisks (*) indicate a significant difference compared to controls ($P < 0.05$).
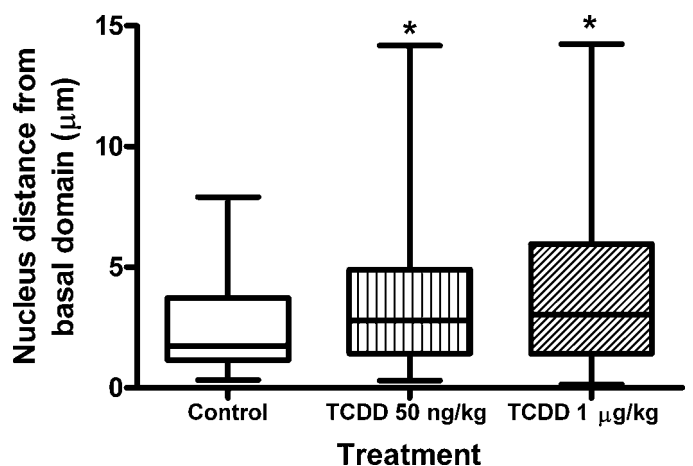
FIG. 5. Maternal TCDD exposure modifies f-actin organization in preimplantation embryos. Eight- to 16-cell embryos (**A**, **B**, and **D**–**G**) and blastocysts (**C** and **H**) were collected from control female rats (**A**–**D**) and rats exposed chronically (**E**–**G**) or acutely (**H**) to TCDD and stained for visualization f-actin. TCDD treatment resulted in cytoplasmic vesicles and f-actin aggregates (**E** and **F**), vacuoles (**H**), and disruption of adherence properties between blastomeres (**G**, arrows). These features were not apparent in control embryos (**A**–**H**). Bar = 20 μm (**A**, **C**, **E**, and **H**) or 10 μm (**B**, **D**, **F**, and **G**).
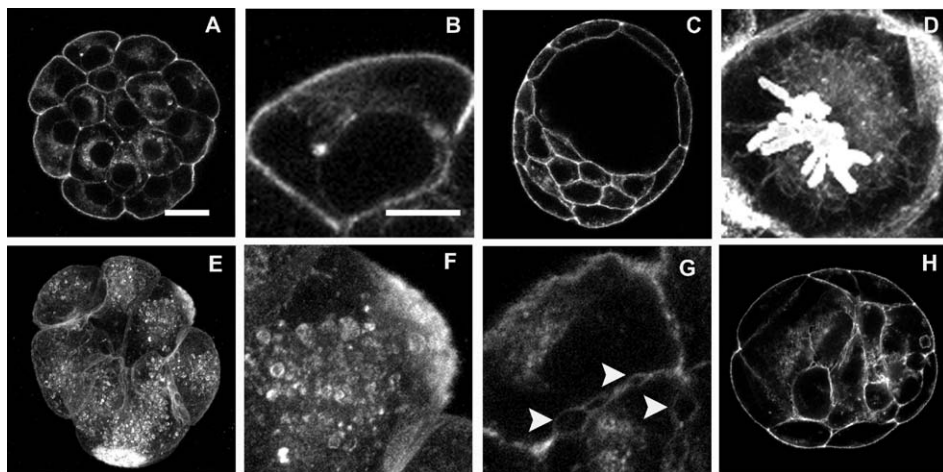
and 4.2 μm from the basal domain of the cell for control, 50 ng/kg of TCDD, and 1 μg/kg of TCDD groups, respectively ($P < 0.05$) (Fig. 4).

### Acute and Chronic TCDD Exposure Modifies the f-actin Organization in 8- to 16-Cell and Blastocyst-Stage Rat Pre-Embryos

Given the role of microfilaments in maintaining cytoplasmic organization, we next evaluated the organization of f-actin in control and TCDD-treated pre-embryos. In interphase blastomeres of control 8- to 16-cell pre-embryos, f-actin was localized as a perinuclear ring with a prominent band of staining that extended from the nuclear surface toward the apical plasma membrane (Fig. 5, A and B). This internal manifestation of polarity was accompanied by prominent subcortical f-actin, consistent with the appearance of intercellular junctions during the process of compaction (Fig. 5, A and B). In control blastocysts, TE cells retained submembranous f-actin localization at the blastomere outer surface (Fig. 5C). In ICM, f-actin labeling was evenly distributed around the nucleus as well as at cell boundaries (Fig. 5C). Interestingly, f-actin was found as a sheath-like structure that surrounded mitotic spindles during the M phase in 8- to 16-cell embryos and in the early blastocyst (Fig. 5D).

Polarization of cytoplasmic f-actin was still observed in 8- to 16-cell embryos exposed both chronically and acutely to TCDD. However, whereas effects at the acute low dose were infrequently observed, all embryos from the acute high-dose and chronic treatment groups exhibited evidence of f-actin disruption: Blastomeres exhibited cytoplasmic vesicles and f-actin aggregates (Fig. 5, E and F). In addition, chronic exposure to TCDD resulted in disruption of f-actin at cell boundaries, indicated by an irregular f-actin profile and the presence of gaps between blastomeres in compacted pre-embryos (Fig. 5G, arrows). Untreated control embryos did not exhibit either of these characteristics. Acutely exposed early blastocysts also exhibited disrupted f-actin localization, and although discrete and tightly apposed f-actin boundaries were observed between TE cells of treated blastocysts, f-actin staining within the ICM appeared to be diffuse and disorganized (Fig. 5H). Additionally, vacuoles were observed in TE and ICM (Fig. 5H). These findings indicate that embryos retrieved from TCDD-exposed animals, when compared to controls, exhibit varying degrees of disorganization in the f-actin cytoskeleton that may underlie the disruptions in nuclear position and centrosome organization noted earlier.

## DISCUSSION

Between the time of ovulation and implantation, mammalian oocytes and embryos, respectively, undergo key modifications in both cell-cycle control and chromatin structure. This critical window of mammalian development is sensitive to perturbations in metabolism, diet, and exposure to environmental toxicants, and effects realized during this period impact the gestational and postgestational health of offspring [26–28]. One of the major defects thought to originate either during oocyte meiotic maturation or mitotic cleavages of the early embryo is the failure to properly align and segregate chromosomes (karyokinesis) coincident with the partitioning of cytoplasm during cytokinesis [29]. Errors in chromosome segregation and cytokinesis are often attributed to cytoskeletal defects, because these processes are especially dependent on tubulin-based microtubules and actin-based microfilaments or their associated motor molecules. We have previously shown that maternal exposure to the environmental toxicant TCDD induces monopolar spindle formation and defects in chromosome segregation and karyokinesis in preimplantation embryos [24]. In the present study, we investigated the hypothesis that alterations in the number and position of interphase TUBG1 foci are also associated with the monopolar spindle formation and cytoskeletal defects observed in embryos following maternal TCDD exposure.

We first analyzed TUBG1 localization in control embryos to determine the normal pattern of expression in rats. An early study in mouse embryos reported that TUBG1 aggregates first appear in interphase cells at the 32-cell stage and that centrioles do not appear until the 64-cell stage [2]. However, more recent studies have demonstrated the presence of perinuclear TUBG1 foci in interphase blastomeres as early as the 2-cell stage in mouse embryos [30]. Our data are consistent with this latter finding in that discrete perinuclear TUBG1 foci were detected in interphase blastomeres of 8- to 16-cell rat embryos. Meiotic and early embryonic mitotic spindles have traditionally been described as being barrel-shaped and nonastral, with the spindle becoming progressively more pointed with each subsequent cell cycle [31]. Whereas the functional significance of the switch from barrel-shaped to pointed spindles is not clear, it may reflect the transition from TUBG1-based microtubule organizing center nucleation of microtubules to nucleation driven by centrioles. In the current study, the analysis of mitotic blastomeres shows that spindles in 8- to 16-cell rat pre-embryos and blastocysts are pointed, which is typical of centriolar microtubule nucleation. However, further work using centriole-specific antibodies and electron micros-

copy is necessary to confirm this. We also found TUBG1 to be distributed along the spindle microtubules. In this regard, TUBG1 has been localized along the spindle microtubules at metaphase I in pig oocytes [32] and along mitotic spindle microtubules in cleavage-stage mouse embryos [2]. It is possible that spindle-associated TUBG1 plays an important role in spindle function by acting as a scaffold for the recruitment of signaling proteins [33].

The localization of TUBG1 during early embryogenesis in rats was essentially the same as that reported previously for other species, but both chronic and acute maternal exposure to TCDD resulted in the displacement of TUBG1 foci from the nucleus to the cortex. The relative position of the nucleus and centrosome define the axis of division and establish cytoplasmic polarity, which is essential for the generation of ICM and TE lineages [34]. Moreover, localization of two TUBG1 foci to opposite sides of the nucleus is a prerequisite for bipolar spindle assembly, which in turn is required for chromosome segregation and maintenance of genome integrity. Consequently, disturbances in the localization and functionality of TUBG1 of the kind described here could have severe developmental outcomes if they persist. Studies of mice deficient in TUBG1 have very clearly illustrated the importance of this protein during development [35]. $Tubg^{-/-}$ mice die before implantation, but careful analysis of early embryogenesis revealed that mitotic arrest frequently occurred at the morula stage, with most cells at the blastocyst stage showing disorganized mitotic spindle-like structures. Moreover, mitotic blastomeres often exhibited a single pericentrin focus and poorly aligned chromosomes [35]. These findings demonstrate an essential role for TUBG1 in microtubule nucleation and/or organization during early embryogenesis. The present study also indicates that normal mitosis is achieved during the first few cleavage divisions by utilizing the maternally inherited supply of TUBG1. Interestingly, both in the current study and in our previous report [24], the negative effects of TCDD on spindle morphology and cytoskeletal architecture were considerably less pronounced at the blastocyst stage when compared to the morula stage. However, it is not known if the earlier defects had a long-lasting impact on embryonic development that could not be measured by the morphological parameters used in the present study. The apparent restoration of normal spindle morphology may result from the utilization of newly expressed embryonic TUBG1, as opposed to maternally derived TUBG1. Alternatively, it may be caused by the de novo synthesis of centrioles upon activation of the embryonic genome. Distinguishing between these possibilities would not be straightforward, because parthenogenetic embryos are capable of generating centrioles de novo and because differentiating between maternal or zygotic TUBG1 would require selective depletion of the latter. Nonetheless, these results reinforce the importance of studying lesions in early development affecting maternally inherited proteins that are rectified by the blastocyst stage of development.

In addition to fragmentation of TUBG1 foci, TCDD exposure resulted in nuclear displacement and monopolar spindles. The specific mechanisms by which TCDD exerts these effects, either via the AHR or independently, are unknown. However, recent evidence suggests that TCDD may alter the function of cytoskeletal proteins by changing posttranslational modifications [36]. In particular, β-actin was differently glycosylated, and the microtubule-associated protein 1S (MAP1S) and actin-related protein 1 (ARP1) homolog A showed enhanced tyrosine phosphorylation when cells were exposed to TCDD. MAP1S colocalizes with centrosomes, and its depletion causes centrosome fragmentation. Consequently,

MAP1S is critically important to the formation of spindle bipoles during mitosis [37–39]. Dallol et al. [40] showed that depletion of MAP1S results in unstable metaphase plate, premature sister chromatid separation, lagging chromosomes, and multipolar spindles. ARP1 is a component of dynactin, a complex that binds microtubules and dynein [41, 42]. Dynactin is involved in endoplasmic reticulum to Golgi transport, the centripetal movement of lysosomes and endosomes, spindle formation, chromosome movement, and nuclear positioning [42]. The expression levels of proteins in cytoskeletal organization and biogenesis, actin filament-based processes, protein transport, and folding have also been shown to be altered by TCDD exposure during osteoblast differentiation from mesenchymal stem cells [43]. Thus, the cytoplasmic disorganization and mitotic defects observed in compaction-stage embryos following maternal exposure to TCDD may be the result of disrupted expression or posttranslational modification to cytoskeleton-related proteins. Further work is required to determine if this is the case.

The mechanisms by which maternal exposures cause nonlethal changes during compaction remain unexplained, but the long-term impact of such perturbations in cell-cycle control and cell polarity on offspring health reveals a serious gap in our understanding of the link between quality of the oocyte and that of the embryo. Not surprisingly, defects in γ-tubulin organization underscore the prevalence of mitotic errors described in human embryos produced by in vitro fertilization [44]. Abnormal microtubule organizing center distribution has been linked to aberrant spindle formation and malsegregation of chromosomes in slow-growing and arrested human cleavage-stage embryos [45, 46]. Additionally, abnormalities that occur early but that do not result in growth arrest have the potential to impact a large proportion of the developing embryo, because the embryo does not appear to be able to eliminate defective blastomeres by apoptosis until the blastocyst stage [47]. The present results clearly indicate that the maturation and function of centrosomes in the early rat embryo is at risk following exposure and likely accounts for overt defects in the processes of cytokinesis and karyokinesis. Moreover only a single, periconceptional exposure was necessary for the effect to be observed. How oocytes respond to agents like TCDD or other toxins to effect disruption of the nuclear-cytoplasmic dialogue in early development represents an important course of future investigation.

In sum, we have shown that TUBG1 foci number and localization are modified in compaction-stage embryos after maternal exposure to the environmental toxicant TCDD. The misregulation of TUBG1 may underpin the defects observed in karyokinesis and cytokinesis that are commonly observed in treated rat blastomeres. Moreover, the extent to which the centrosome nuclear interaction observed here impacts key epigenetic alterations in chromatin structure and function is deserving of further study.

## REFERENCES

1. Szollosi D, Calarco P, Donahue RP. Absence of centrioles in the first and second meiotic spindles of mouse oocytes. J Cell Sci 1972; 11:521–541.
2. Gueth-Hallonet C, Antony C, Aghion J, Santa-Maria A, Lajoie-Mazenc I, Wright M, Maro B. Gamma-tubulin is present in acentriolar MTOCs during early mouse development. J Cell Sci 1993; 105(pt 1):157–166.
3. Zheng Y, Wong ML, Alberts B, Mitchison T. Nucleation of microtubule assembly by a gamma-tubulin-containing ring complex. Nature 1995; 378:578–583.
4. Wiese C, Zheng Y. A new function for the gamma-tubulin ring complex as a microtubule minus-end cap. Nat Cell Biol 2000; 2:358–364.
5. Joshi HC, Palacios MJ, McNamara L, Cleveland DW. Gamma-tubulin is a

centrosomal protein required for cell cycle-dependent microtubule nucleation. Nature 1992; 356:80–83.

6. Oakley BR, Oakley CE, Yoon Y, Jung MK. Gamma-tubulin is a component of the spindle pole body that is essential for microtubule function in *Aspergillus nidulans*. Cell 1990; 61:1289–1301.

7. Vardy L, Fujita A, Toda T. The gamma-tubulin complex protein Alp4 provides a link between the metaphase checkpoint and cytokinesis in fission yeast. Genes Cells 2002; 7:365–373.

8. Oakley BR. Gamma-tubulin. Curr Top Dev Biol 2000; 49:27–54.

9. Paluh JL, Nogales E, Oakley BR, McDonald K, Pidoux AL, Cande WZ. A mutation in gamma-tubulin alters microtubule dynamics and organization and is synthetically lethal with the kinesin-like protein pkl1p. Mol Biol Cell 2000; 11:1225–1239.

10. Hendrickson TW, Yao J, Bhadury S, Corbett AH, Joshi HC. Conditional mutations in gamma-tubulin reveal its involvement in chromosome segregation and cytokinesis. Mol Biol Cell 2001; 12:2469–2481.

11. Doxsey SJ. Molecular links between centrosome and midbody. Mol Cell 2005; 20:170–172.

12. Doxsey S, Zimmerman W, Mikule K. Centrosome control of the cell cycle. Trends Cell Biol 2005; 15:303–311.

13. Kuriyama R, Borisy GG. Microtubule-nucleating activity of centrosomes in Chinese hamster ovary cells is independent of the centriole cycle but coupled to the mitotic cycle. J Cell Biol 1981; 91:822–826.

14. Hinchcliffe EH, Li C, Thompson EA, Maller JL, Sluder G. Requirement of Cdk2-cyclin E activity for repeated centrosome reproduction in *Xenopus* egg extracts. Science 1999; 283:851–854.

15. Matsumoto Y, Hayashi K, Nishida E. Cyclin-dependent kinase 2 (Cdk2) is required for centrosome duplication in mammalian cells. Curr Biol 1999; 9:429–432.

16. Kuriyama R, Borisy GG. Centriole cycle in Chinese hamster ovary cells as determined by whole-mount electron microscopy. J Cell Biol 1981; 91:814–821.

17. Tsou MF, Stearns T. Mechanism limiting centrosome duplication to once per cell cycle. Nature 2006; 442:947–951.

18. Tsou MF, Stearns T. Controlling centrosome number: licenses and blocks. Curr Opin Cell Biol 2006; 18:74–78.

19. Birnbaum LS. Developmental effects of dioxins and related endocrine disrupting chemicals. Toxicol Lett 1995; 82–83:743–750.

20. Bock KW, Kohle C. Ah receptor: dioxin-mediated toxic responses as hints to deregulated physiologic functions. Biochem Pharmacol 2006; 72: 393–404.

21. Knerr S, Schrenk D. Carcinogenicity of 2,3,7,8-tetrachlorodibenzo-*p*-dioxin in experimental models. Mol Nutr Food Res 2006; 50:897–907.

22. Rowlands JC, Gustafsson JA. Aryl hydrocarbon receptor-mediated signal transduction. Crit Rev Toxicol 1997; 27:109–134.

23. Enan E, Matsumura F. Evidence for a second pathway in the action mechanism of 2,3,7,8-tetrachlorodibenzo-*p*-dioxin (TCDD). Significance of Ah-receptor mediated activation of protein kinase under cell-free conditions. Biochem Pharmacol 1995; 49:249–261.

24. Hutt KJ, Shi Z, Albertini DF, Petroff BK. The environmental toxicant 2,3,7,8-tetrachlorodibenzo-*p*-dioxin disrupts morphogenesis of the rat pre-implantation embryo. BMC Dev Biol 2008; 8:1–12.

25. Combelles CM, Cekleniak NA, Racowsky C, Albertini DF. Assessment of nuclear and cytoplasmic maturation in in vitro matured human oocytes. Hum Reprod 2002; 17:1006–1016.

26. Wynn M, Wynn A. Nutrition around conception and the prevention of low birth weight. Nutr Health 1988; 6:37–52.

27. Barker DJ, Gluckman PD, Robinson JS. Conference report: fetal origins of adult disease—report of the First International Study Group, Sydney, 29–30 October 1994. Placenta 1995; 16:317–320.

28. Kwong WY, Wild AE, Roberts P, Willis AC, Fleming TP. Maternal undernutrition during the preimplantation period of rat development causes blastocyst abnormalities and programming of postnatal hypertension. Development 2000; 127:4195–4202.

29. Vogt E, Kirsch-Volders M, Parry J, Eichenlaub-Ritter U. Spindle formation, chromosome segregation and the spindle checkpoint in mammalian oocytes and susceptibility to meiotic error. Mutat Res 2008; 651:14–29.

30. Meng XQ, Fan HY, Zhong ZS, Zhang G, Li YL, Chen DY, Sun QY. Localization of gamma-tubulin in mouse eggs during meiotic maturation, fertilization, and early embryonic development. J Reprod Dev 2004; 50: 97–105.

31. Schatten G, Simerly C, Schatten H. Microtubule configurations during fertilization, mitosis, and early development in the mouse and the requirement for egg microtubule-mediated motility during mammalian fertilization. Proc Natl Acad Sci U S A 1985; 82:4152–4156.

32. Lee J, Miyano T, Moor RM. Spindle formation and dynamics of gamma-tubulin and nuclear mitotic apparatus protein distribution during meiosis in pig and mouse oocytes. Biol Reprod 2000; 62:1184–1192.

33. Ma W, Koch JA, Viveiros MM. Protein kinase C delta (PKCdelta) interacts with microtubule organizing center (MTOC)-associated proteins and participates in meiotic spindle organization. Dev Biol 2008; 320: 414–425.

34. Cowan CR, Hyman AA. Asymmetric cell division in *C. elegans*: cortical polarity and spindle positioning. Annu Rev Cell Dev Biol 2004; 20: 427–453.

35. Yuba-Kubo A, Kubo A, Hata M, Tsukita S. Gene knockout analysis of two gamma-tubulin isoforms in mice. Dev Biol 2005; 282:361–373.

36. Kim JH, In YJ, Kim WK, Bae KH, Kang S, Lee SC. Differential signatures of protein glycosylation and phosphorylation in human Chang liver cells induced by TCDD treatment. Toxicol Lett 2008; 178:20–28.

37. Orban-Nemeth Z, Simader H, Badurek S, Trancikova A, Propst F. Microtubule-associated protein 1S, a short and ubiquitously expressed member of the microtubule-associated protein 1 family. J Biol Chem 2005; 280:2257–2265.

38. Song MS, Chang JS, Song SJ, Yang TH, Lee H, Lim DS. The centrosomal protein RAS association domain family protein 1A (RASSF1A)-binding protein 1 regulates mitotic progression by recruiting RASSF1A to spindle poles. J Biol Chem 2005; 280:3920–3927.

39. Ding J, Valle A, Allen E, Wang W, Nardine T, Zhang Y, Peng L, Yang Y. Microtubule-associated protein 8 contains two microtubule binding sites. Biochem Biophys Res Commun 2006; 339:172–179.

40. Dallol A, Cooper WN, Al-Mulla F, Agathanggelou A, Maher ER, Latif F. Depletion of the Ras association domain family 1, isoform A-associated novel microtubule-associated protein, C19ORF5/MAP1S, causes mitotic abnormalities. Cancer Res 2007; 67:492–500.

41. Muhua L, Karpova TS, Cooper JA. A yeast actin-related protein homologous to that in vertebrate dynactin complex is important for spindle orientation and nuclear migration. Cell 1994; 78:669–679.

42. Schroer TA. Dynactin. Annu Rev Cell Dev Biol 2004; 20:759–779.

43. Carpi D, Korkalainen M, Airoldi L, Fanelli R, Hakansson H, Muhonen V, Tuukkanen J, Viluksela M, Pastorelli R. Dioxin-sensitive proteins in differentiating osteoblasts: effects on bone formation in vitro. Toxicol Sci 2009; 108:330–343.

44. Chatzimeletiou K, Morrison EE, Prapas N, Prapas Y, Handyside AH. The centrosome and early embryogenesis: clinical insights. Reprod Biomed Online 2008; 16:485–491.

45. Chatzimeletiou K, Rutherford AJ, Griffin DK, Handyside AH. Is the sperm centrosome to blame for the complex polyploid chromosome patterns observed in cleavage stage embryos from an OAT patient? Zygote 2007; 15:81–90.

46. Chatzimeletiou K, Morrison EE, Prapas N, Prapas Y, Handyside AH. Spindle abnormalities in normally developing and arrested human preimplantation embryos in vitro identified by confocal laser scanning microscopy. Hum Reprod 2005; 20:672–682.

47. Brison DR, Schultz RM. Apoptosis during mouse blastocyst formation: evidence for a role for survival factors including transforming growth factor alpha. Biol Reprod 1997; 56:1088–1096.